Supporting Material

1. Schematics of the pilot system.

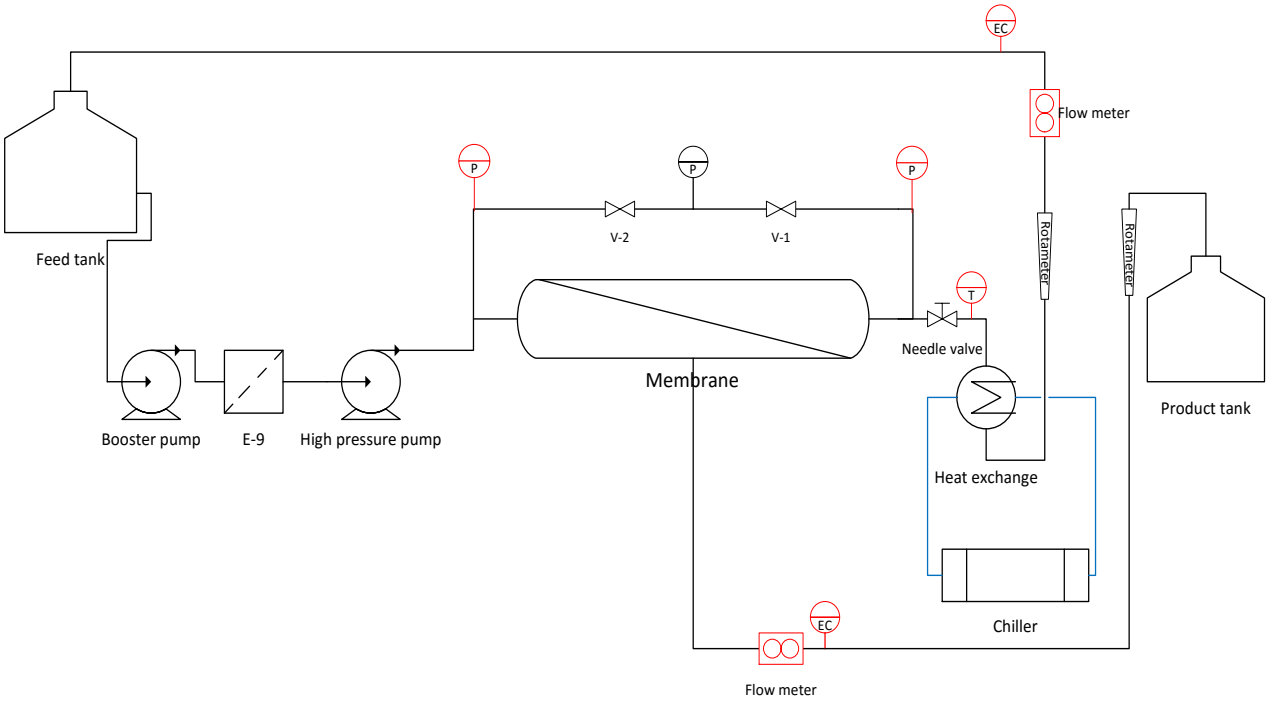

Figure S1 - Schematics of the pilot system comprising of a single 4″ membrane module.

Figure S1 describe the experimental reverse osmosis system used for this study. The system can be operated either full recirculation mode where both retentate and permeate are recirculated back to the feed tank, or semi-recirculation mode, where the permeate is collected to a different tank. The latter mode is used to simulate high permeate recovery ratios in the 1st and 2nd pass as obtained in real-life operations. For this purpose, commercial desalination plants mostly utilize membranes in serious which function in a once-through mode (a membrane train). This operation mode is different from the semi-circulation mode by two major aspects: 1. In recirculation mode the cross-flow velocity is approximately constant while in once-through mode it decreases with the recovery

ratio; 2. In recirculation mode the pressure is approximately constant while in once-through mode there's a pressure-drop of typically 1.5-2 bars for the entire membrane train. These differences are fully accounted for in the simulation code and it is easy to switch between operational modes.

2. Description of the sub algorithm for predicting water flux and salt concentrations

For every recovery segment, Eq. S1-S3 are solved, producing the water flux (*Jv*), the salt concentration in the film layer (*Cm*) and the NaCl concentration in the permeate (*Cp*).

$$J_{v,i} = P_w(P - \phi_m C_{m,i} RT) \tag{S1}$$

$$J_{v,i} C_{p,i} = P_{salt}(C_{m,i} - C_{p,i}) \tag{S2}$$

$$C_{m,i} - C_{p,i} = (C_{b,i} - C_{p,i}) e^{J_{v,i}/k_{s,i}} \tag{S3}$$

The osmotic coefficient in the film layer ϕ_m is obtained from PHREEQC, as using the Pitzer approach enables an accurate calculation of this parameter as a function of solution composition. Since the composition of the film layer is primarily unknown, the bulk composition is used as an initial guess. Eq. S1-S3 are then solved again, and the process repeats itself until ϕ_m converges. Subsequently, the bulk salt concentration for the next segment is calculated by mass balance.

$$C_{b,i+1} = [C_{b,i}(1 - r_i) - drC_{p,i}] / (1 - r_{i+1}) \tag{S4}$$

In Eq. S4, *r* is the local recovery ratio, while *dr* is the numerical step size (default is 0.01 = 1% recovery). The permeability constants of the membrane for water (P_w) and salt (P_s) appearing in Eq. S1-S3 can be either received as direct input or estimated by the program based on manufacturer

data obtained at standard test conditions. The permeability constants are then corrected for temperature as shown in Eq. S5-S6, from [1]

$$P_w = P_{w,25^0C} e^{0.0093(T-298.15)} \quad \text{(S5)}$$

$$P_s = P_{s,25^0C} e^{0.0483(T-298.15)} \quad \text{(S6)}$$

The mass transfer coefficient for salt (k) can also be inserted manually or estimated by the program using a widely used empirical correlation for spiral-wound (Schock and Miquel, 1987).

$$k_s = 0.065 D d_H^{-1} (\rho u d_H \mu^{-1})^{0.875} (\mu \rho^{-1} D^{-1})^{0.25} \quad \text{(S7)}$$

The density (ρ) is obtained from PHREEQC as a function of the solution composition, which is another exclusive feature of the Pitzer approach. The diffusion coefficient of NaCl (D_{NaCl}) is calculated by Eq. S8 taken from (Taniguchi et al., 2001),

$$D_{NaCl,i} = 6.725 \cdot 10^{-6}\, \mathrm{e}^{0.0001546 S_i - 2513/T} \quad \text{(S8)}$$

while the viscosity is calculated according to the formulation suggested in (Altaee, 2012).

3. Experimental results and calculation of transport coefficients

The results of the low recovery low pH transport constants experiments are shown in Table S1 for the three membranes used. The bulk salt concentrations and boric-acid concentrations presented were calculated as the average concentration of the feed and brine streams, representing the average concentration over the membrane element. The expected trends of increased permeate flux and boric-acid rejection as the pressure was increased were observed with both membranes. The rejection of seawater salts also increased with the pressure, as expected, while the conductivity rejection by the brackish water element increased through the low pressure region, but decreased

at the higher pressure range, suggesting high concentration polarization conditions for NaCl as further discussed below.

The problem of fitting model parameters to empirical results was translated into a non-linear optimization problem following the least-square procedure. The optimization problem was solved using Python [6], a free programming platform with powerful numerical functions. The solver used (fmin), is based on the Nedler-Mead Simplex algorithm, which is included in the Scipy library (optimize toolbox).

Table S1 - RO filtration results for the transport constant experiments. Mediterranean seawater were used as feed. Salt concentrations are the sum of all ions in solution. Data highlighted in red was removed from the analysis

P (bar)	J_v (m/s)	Bulk salt (M)	Permeate salt (M)	Bulk $B(OH)_3$ (M)	Permeate $B(OH)_3$ (M)
			HRLE		
29.1	1.22E-06	1.066	0.0295	3.44E-04	2.35E-04
32.2	1.78E-06	1.078	0.0204	3.62E-04	1.97E-04
34.7	2.26E-06	1.134	0.0164	3.76E-04	1.81E-04
36	2.48E-06	1.106	0.0152	3.65E-04	1.71E-04
37.5	2.81E-06	1.125	0.0164	3.61E-04	1.66E-04
39.9	3.25E-06	1.127	0.0137	3.70E-04	1.52E-04
43	3.84E-06	1.108	0.0122	3.69E-04	1.44E-04
46.6	4.36E-06	1.114	0.0112	3.67E-04	1.32E-04
50	4.87E-06	1.094	0.0102	3.61E-04	1.22E-04
			SWC6		
32.51	1.093E-06	1.09	2.91E-02	3.51E-04	3.07E-04
34.73	1.717E-06	1.25	1.75E-02	4.11E-04	2.45E-04
36.16	2.416E-06	1.26	1.23E-02	4.19E-04	2.00E-04
38.47	2.422E-06	1.28	9.83E-03	4.23E-04	1.70E-04
40.64	3.811E-06	1.29	8.09E-03	4.21E-04	1.47E-04
42.67	4.321E-06	1.29	6.97E-03	4.28E-04	1.27E-04
44.34	4.77E-06	1.29	6.36E-03	4.32E-04	1.18E-04
46.12	5.407E-06	1.30	5.69E-03	4.28E-04	1.10E-04

50.05	6.795E-06	1.31	4.94E-03	4.32E-04	9.29E-05
			ESPA2		
5.14	4.08E-06	4.19E-02	1.14E-03	3.49E-04	3.13E-04
5.95	5.06E-06	4.20E-02	1.13E-03	3.50E-04	3.09E-04
7.12	6.33E-06	4.27E-02	1.19E-03	3.50E-04	3.04E-04
8.11	7.23E-06	4.28E-02	1.30E-03	3.51E-04	2.99E-04
9.12	8.44E-06	4.30E-02	1.08E-03	3.51E-04	2.98E-04
10.02	9.38E-06	4.37E-02	1.11E-03	3.52E-04	2.97E-04
11.08	1.05E-05	4.31E-02	1.14E-03	3.53E-04	2.95E-04
12.11	1.10E-05	4.34E-02	1.20E-03	3.53E-04	2.94E-04
13.01	1.21E-05	4.39E-02	1.15E-03	3.54E-04	2.94E-04

The results listed in Table S1 was used to calculate the constants required by the SDF (k_{BOH3}, $Ps_{B(OH)3}$) and SKF (k_{BOH3}, $Ps_{B(OH)3}$ and $\sigma_{B(OH)3}$) models by non-linear optimization. The boric-acid transport equations, combined with the film model equation and rearranged, yielded Eq. (S9) For the SDF model and Eq. (S10) for the SKF model.

$$\frac{C_b - C_p}{C_p} = \frac{J_v}{P_{B(OH)_3} e^{J_v/k}} \tag{S9}$$

$$\frac{C_{bi} - C_{pi}}{C_{pi}} - \frac{\sigma}{1-\sigma}\left(1 - e^{-J_{vi}(1-\sigma/P_s)}\right)e^{-J_{vi}/k} \tag{S10}$$

Accordingly, the optimization problems was solved by non-linear optimization are described by Eqs. (S11) and (S12) for SDF and SKF, respectively.

$$Minimize\left\{\sum_{i=1}^{n}\left(\frac{C_{bi} - C_{pi}}{C_{pi}} - \frac{J_{vi}}{P_s e^{J_{vi}/k}}\right)^2\right\} \tag{S11}$$

$$Minimize\left\{\sum_{i=1}^{n}\left(\frac{C_{bi} - C_{pi}}{C_{pi}} - \frac{\sigma}{1-\sigma}\left(1 - e^{-J_{vi}(1-\sigma/P_s)}\right)e^{-J_{vi}/k}\right)^2\right\} \tag{S12}$$

The overall average transport of charged solutes (salt) required by the *WATRO* model was determined by the osmotic pressure method as follows: first the water permeability was determined by experimental results with DI water, according to Eq. S13

$$P_W = \frac{J_V}{\Delta p} \tag{S13}$$

Then, from the experimental results shown in table 1, the concentration near the membrane wall (C_m) is calculated as follows:

$$C_m = \frac{1}{\phi_m}\left[\phi_P C_p - \frac{1}{RT}\left(\frac{J_V}{P_W} - \Delta P\right)\right] \tag{S14}$$

Where ϕ is the osmotic coefficient which was calculated for each specific feed composition using the Pitzer model in PHREEQC. k_s was then determined using Eq. S3 from the slope of J_v Vs. $ln\ [(c_m - c_p)/(c_b - c_p)]$ plot, as shown in Fig. S2. P_s was determined using Eq. (S2) from the slope of J_v Vs. $(c_m - c_p)/c_p$ plot, as shown in Fig. S3.

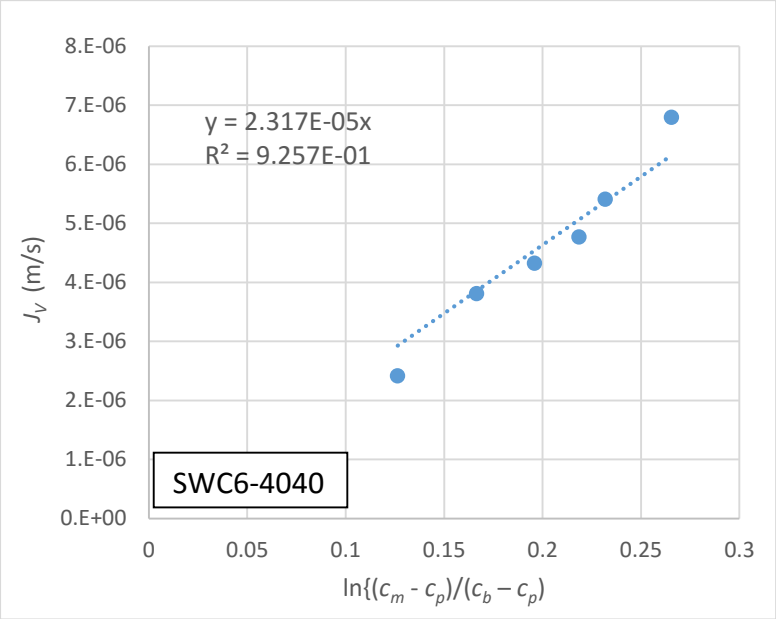

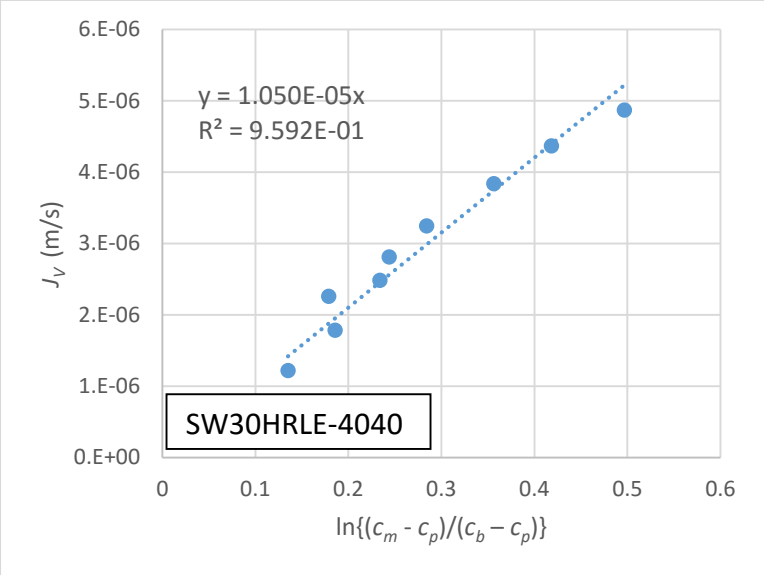

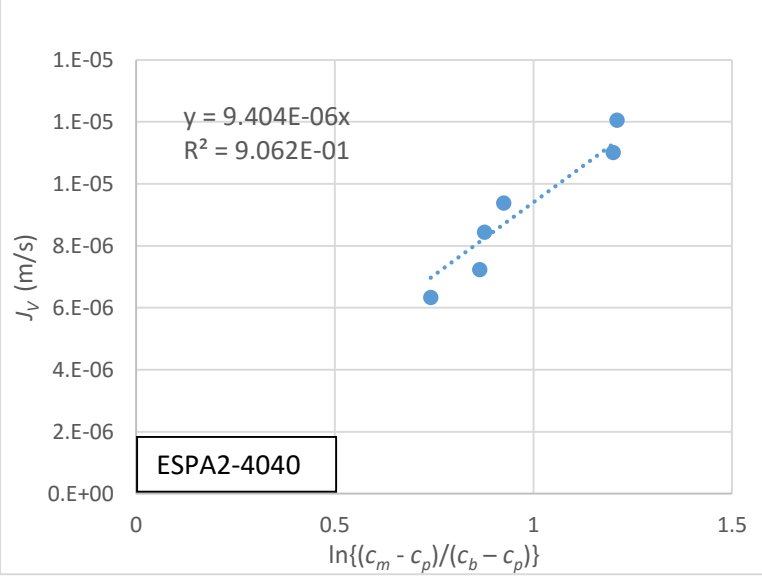

Figure 2S - Linear regression for obtaining the mass transfer coefficient of salt (determined by the slope of the regression) by the osmotic pressure method for the three different membranes.

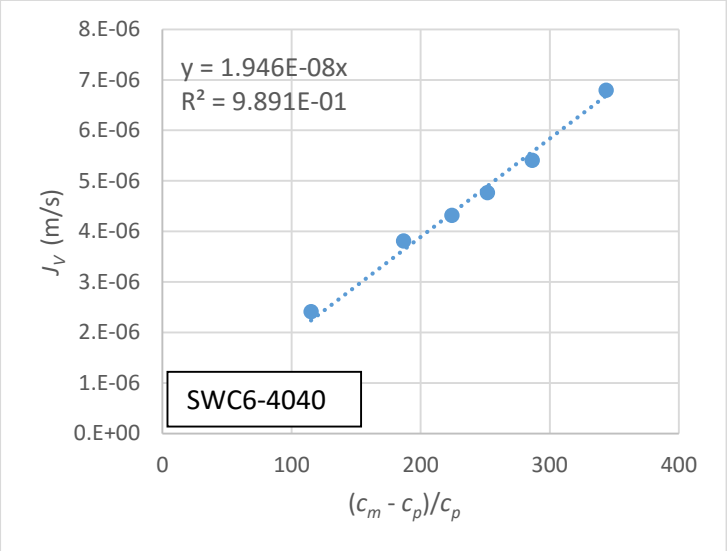
y = 1.946E-08x
R² = 9.891E-01
SWC6-4040
8.E-06
7.E-06
6.E-06
5.E-06
4.E-06
3.E-06
2.E-06
1.E-06
0.E+00
J_V (m/s)
0
100
200
300
400
$(c_m - c_p)/c_p$

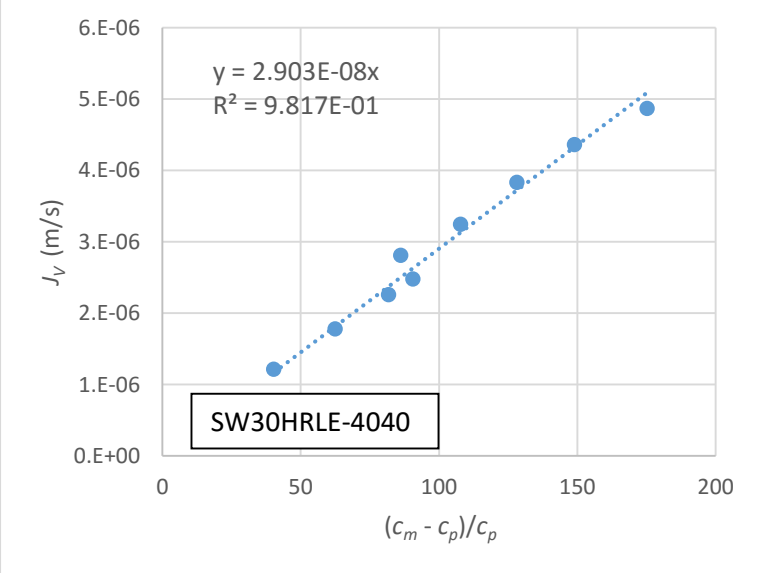
y = 2.903E-08x
R² = 9.817E-01
SW30HRLE-4040
6.E-06
5.E-06
4.E-06
3.E-06
2.E-06
1.E-06
0.E+00
J_V (m/s)
0
50
100
150
200
$(c_m - c_p)/c_p$

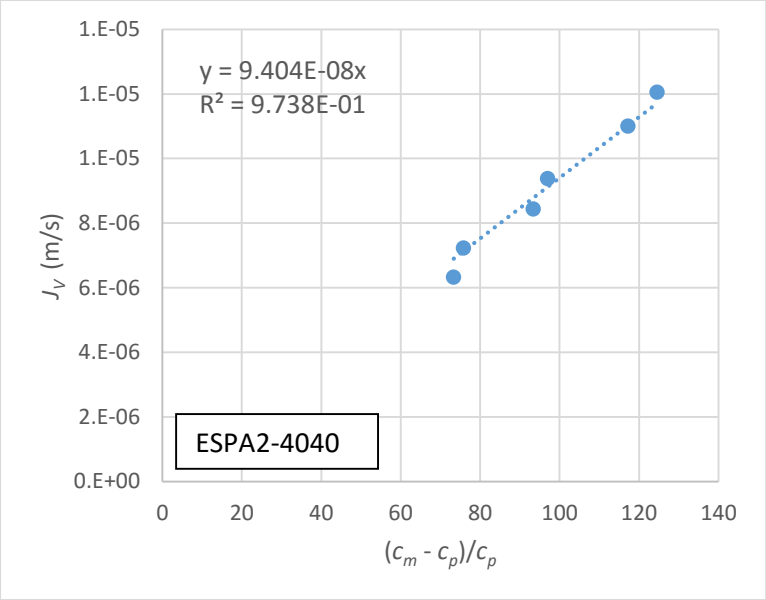

Figure 3S - Linear regression for obtaining the permeability coefficient of salt (determined by the slope of the regression) by the osmotic pressure method for the three different membranes.

4. Water flux and permeate salt concentrations: modeled vs. experimental results

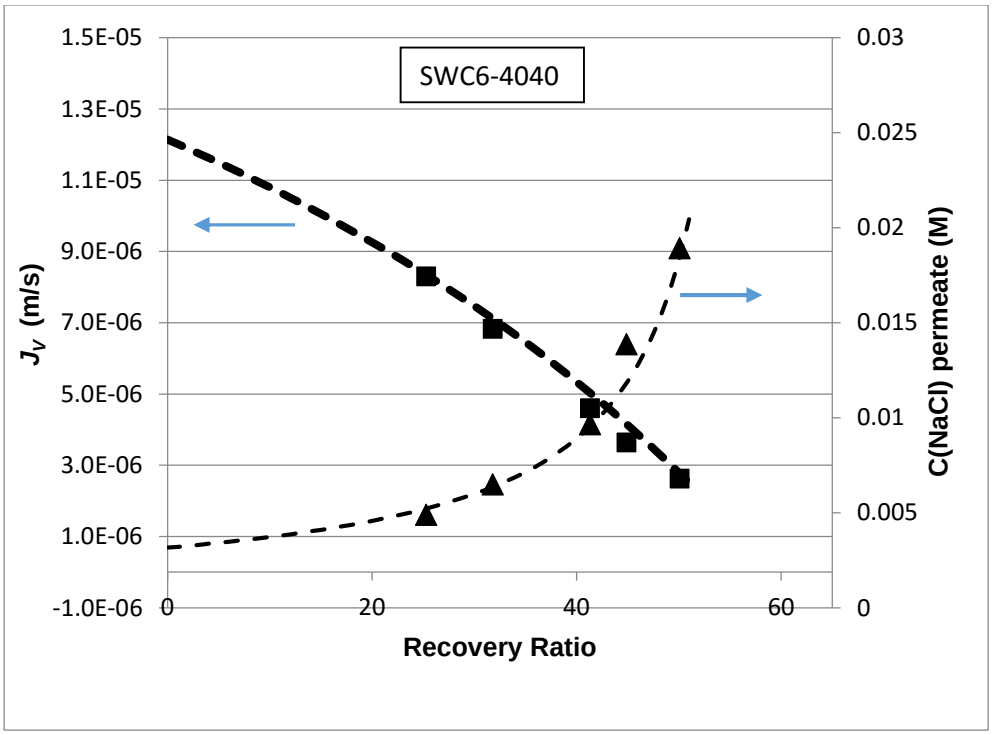
SWC6-4040
1.5E-05
1.3E-05
1.1E-05
9.0E-06
7.0E-06
5.0E-06
3.0E-06
1.0E-06
-1.0E-06
0.03
0.025
0.02
0.015
0.01
0.005
0
0
20
40
60
Recovery Ratio
J_v (m/s)
C(NaCl) permeate (M)

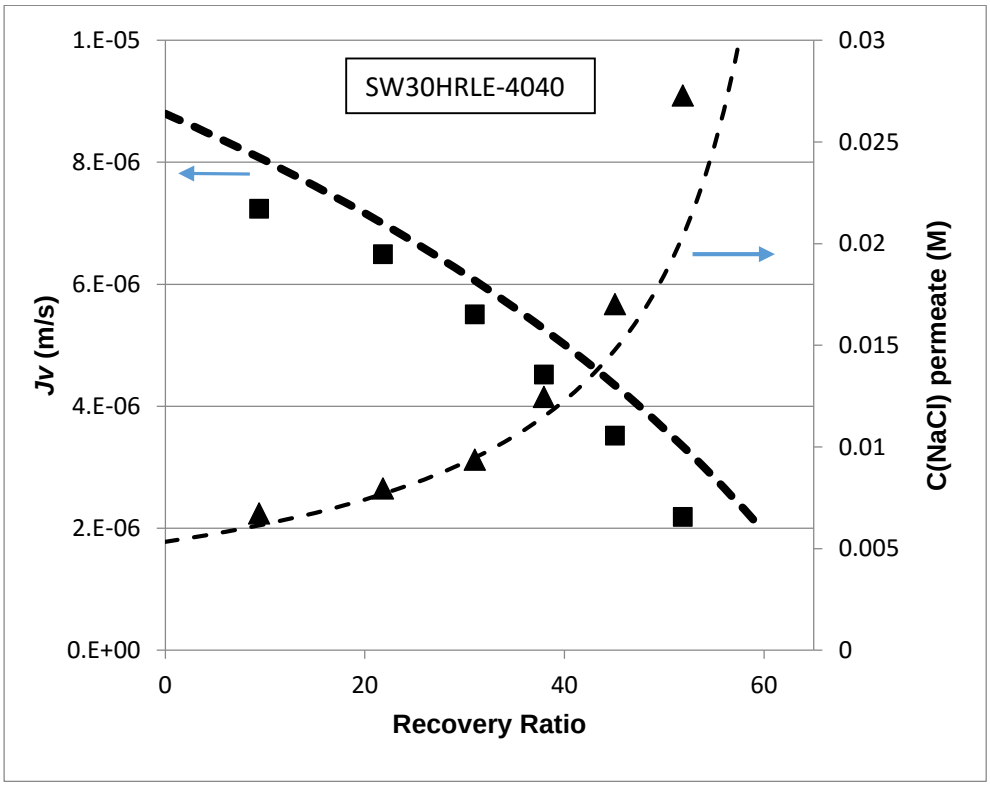
SW30HRLE-4040
1.E-05
8.E-06
6.E-06
4.E-06
2.E-06
0.E+00
0.03
0.025
0.02
0.015
0.01
0.005
0
0
20
40
60
Recovery Ratio
Jv (m/s)
C(NaCl) permeate (M)

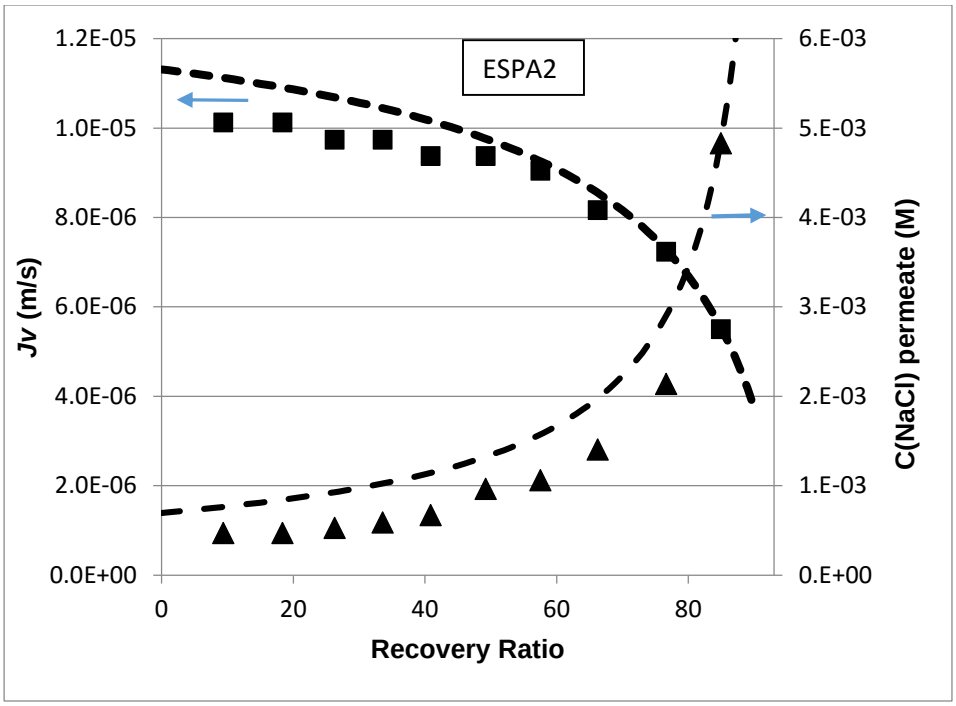

Fig. 4S – Water flux and permeate NaCl concentrations. Experimental results (lines) and projections by *WATRO* (symbols).

5. Correlation for the parameter θ

The parameter θ appearing in Eq. 10 and defined in Eq. 13 adopted from (Nir et al., 2015) is the relative difference between the permeabilities of Na^+ and Cl^-, which are the ions of the dominant salt. As such, θ is influenced by the effective charge within the active layer of the RO membrane. The membrane charge is a function of both pH, which determines the concentration of ionized functional groups and salt concentration, which act to decrease the effective charge, presumably by the binding of counter-ions to some of the ionized groups. At pH ~ 9 all the functional are charged and θ no longer increase with pH, while at low pH (~4.5) these groups are protonated and θ reaches a minimum value. Consequently, plotting θ versus pH should result in an S like function with lower and upper asymptotes as seen in Fig. 5S. A suitable mathematical expression for describing such functions is the so called “logistic function”, which was used here for fitting the experimental results from (Nir et al., 2015).

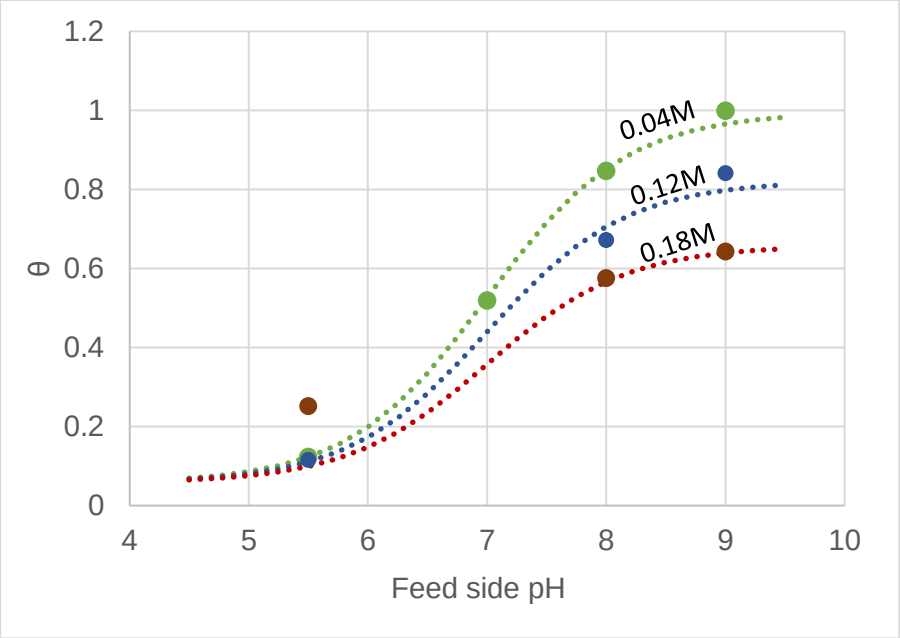

Fig. 5S. Logistic correlation of the θ parameter with respect to pH and NaCl concentration. Experimental results are adopted from (Nir et al., 2015)

$$\theta(pH) = \frac{1 - f(C_s) - a}{1 + e^{-b(pH_m - 7)}} + a \qquad \text{(S15)}$$

$$f(C) = \frac{\Delta\theta_{\max}}{1 + e^{-c(C_m - 0.12)}} \qquad \text{(S16)}$$

Table S2. Parameters from Eqs. S15, S16 fitted to the results from (Nir et al., 2015)

a	b	c	$\Delta\theta_{\max}$
0.057	1.728	52.63	0.357

In Eq. S15, which describes θ as function of pH, 1-$f(C_s)$ is the value of the upper asymptote, which is a function of salt concentration C_s. a is the value of the lower asymptote and b determines the "growth rate of the function". Both a and b are fitting parameters.

Eq. S16, is another logistic function used to describe the reduction in the maximal θ value (the upper asymptote) as a result of increasing salt concentration. Also in this case, the effect of

increasing concentration on the membrane charge and therefore on θ should reach an asymptote at high salt concentration due to the limited sites available for hosting counter-ions within the membrane. This asymptotic behavior was recently described in (Nir et al., 2015) and was found to begin at NaCl concentration of ~0.2M. Since the high NaCl concentration used in (Nir et al., 2015) was similar (0.18M), the maximum reduction in θ measured in (Nir et al., 2015) was used as the upper asymptote. The mid value 0.12M that was used in (Nir et al., 2015) was taken as the mid-point of the function. c in Eq. S16 is a fitting parameter. The values of all parameters used in Eqs. 15-16 are given in table S2

As seen in Fig. S5, all the experimental θ values were well described by th empirical correlation except for a single value at low pH which was considered an outlier and not included in the fitting process. Fitting was done in Python with the function 'fmin'.

6. Boron permeate concentration as a function of recovery

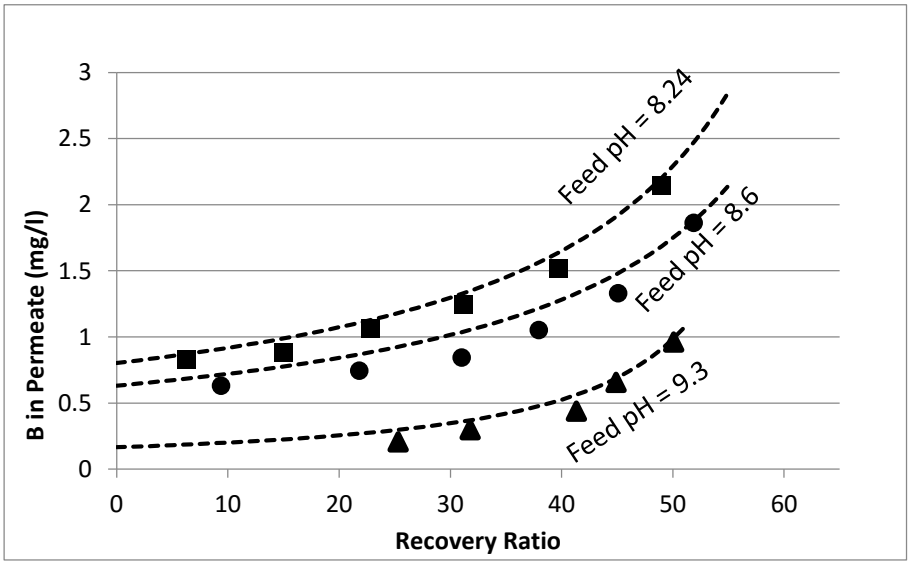

Fig. 6S –boron permeate concentration (local) as a function of recovery. Symbols represent experimental results. Dotted line are predictions by the *WATRO* simulation program. Feed is seawater at three different pH values. Membranes are SW30HRLE-4040 and SWC6 (for feed pH = 9.3)

References

Altaee, A., 2012. Computational model for estimating reverse osmosis system design and performance: Part-one binary feed solution. Desalination 291, 101–105. doi:10.1016/j.desal.2012.01.028

Nir, O., Bishop, N.F., Lahav, O., Freger, V., 2015. Modeling pH Variation in Reverse Osmosis. Water Res. doi:10.1016/j.watres.2015.09.038

Schock, G., Miquel, A., 1987. Mass transfer and pressure loss in spiral wound modules. Desalination 64, 339–352. doi:http://dx.doi.org/10.1016/0011-9164(87)90107-X

Taniguchi, M., Kurihara, M., Kimura, S., 2001. Behavior of a reverse osmosis plant adopting a brine conversion two-stage process and its computer simulation. J. Memb. Sci. 183, 249–257. doi:10.1016/S0376-7388(00)00597-4